*Supporting information*

# Dual-Pathway Sensing in Ti-MOFs for Selective VOCs Discrimination by SERS

Zijing Guo[a], Xiaobing Ren[b], Jiale Hu[a], Yihui Dong[a]*, Wei Cao[b], Suli Liu[a], Zhihui Dai[a,c,d]*

[a]*Nanjing Tech University, School of Chemistry and Molecular Engineering, Nanjing, 211816, P. R. China*

[b]*Nanjing Tech University, State Key Laboratory of Materials-Oriented Chemical Engineering, Nanjing, 211816, P. R. China*

[c]*Collaborative Innovation Centre of Biomedical Functional Materials of Jiangsu Province, School of Chemistry and Materials Science, Nanjing Normal University, Nanjing, 210023, P. R. China*

[d]*State Key Laboratory of Analytical Chemistry for Life Science, Nanjing University, Nanjing, 210023, P. R. China*

**Content sections:**

15. Atomic structure of MIL-125, chloroform, and toluene

## 1. Experimental Section

### 1.1 Materials

Tetrabutyl titanate ($Ti(OC_4H_9)_4$, >99%) was purchased from Shanghai Aladdin Biochemical Technology Co., Ltd. 1,4-benzenedicarboxylic acid ( >99%) was purchased from Shanghai McLean Biochemical Technology Co., Ltd. Anhydrous methanol (MeOH, AR), *N,N*-dimethylformamide (DMF, AR), acetone (AR), chloroform (AR), toluene (AR), zinc chloride ($ZnCl_2$, AR), copper chloride dihydrate ($CuCl_2 \cdot H_2O$, AR), silver nitrate ($AgNO_3$, AR) were purchased from Sinopharm Chemical Reagent Co., Ltd. Manganese chloride tetrahydrate ($MnCl_2$, >99.99%) was purchased from Shanghai Yuanye Biotechnology Co., Ltd. Deionized water was used throughout the experiment, and none of the above tests required further purification and direct use.

### 1.2 Synthesis of Ti-MOF materials

MIL-125, MIL-125-defect, and MIL-125-X were synthesized according to the reported method[30] but with a slight modification. For the preparation of MIL-125, 3.0 g terephthalic acid were mixed with 54 mL and *N, N*-dimethylacetamide (DMF) under stirring for 30 mins, and 6 mL methanol and 1.56 mL tetrabutyl titanate were added under stirring for another 30 mins. The mixture was then heated at 130 °C for 24 h using hydrothermal method. After cooling down to room temperature, the resulting product was collected by centrifugation and washed with DMF and methanol three times, and then dried in a vacuum at 150 ℃ for 12 h to remove solvent molecules. For the preparation of MIL-defect, the same procedure was used as for the synthesis of MIL-125 except from that 1.2 mL of tetrabutyl titanate was used. For the preparation of MIL-125-X, 0.5 g MIL-125-defect was dispersed in 35 mL methanol, then 0.33 mmol metal salt ($CuCl_2 \cdot H_2O$, $ZnCl_2$, $MnCl_2$, respectively) was added (0.1 mmol of $AgNO_3$ is added after adding Cu metal salt to prepare MIL-125-Cu+Ag) and stirred for 3 h. The resulting product was collected by centrifugation and washed with methanol for 3 times and then dried in a vacuum at 100 ℃ for 12 h to remove solvent molecules.

### 1.3 Characterizations

The crystal structure of the sample was obtained by powder X-ray diffraction (XRD, Bruker D8 ADVANCE) and Raman spectroscopy (HORIBA, Japan). The functional group information of the sample was obtained by Fourier transform infrared (FT-IR, Thermo Fisher, Nicolet is 10). The sample was degassed at 120 ℃ for 8h, and its nitrogen adsorption-desorption isotherm was measured at 77K using an ASAP 2460 analyzer for BET surface area and porosity analysis. To elucidate the electron transport capabilities of the sample, the impedance of the material at an open circuit voltage was measured using an Autolab PGSTAT302N at a disc electrode speed of 1400 r/min. The morphology and elemental mapping of the sample were obtained by field emission scanning electron microscopy (SEM, JEOL JSM-IT300). The bandgap was calculated using UV-vis diffuse reflectance spectroscopy measured by a UV-Vis (PerkinElmer Lambda 1050). X-ray photoelectron spectroscopy (XPS, Thermo Scientific K-Alpha) was carried out using a Kratos Axis Ultra Hybrid spectrometer using Al Kα X-rays and data were analyzed using CASAXPS. Photoluminescence (PL, F-4700) measurements were conducted under excitation wavelength at 300 nm, with slit width at 5nm, and test voltage at 600 V.

### 1.4 SERS experiments

Prior to SERS measurements, control Raman spectra were recorded for the pure liquid analytes (chloroform, toluene, dichloromethane, and benzene) at room temperature without any substrate. For the SERS samples, the substrates were prepared as follows: First, appropriate 50 mg MOF powder was removed and placed on a slide, flattened and placed in a sealed gas chamber with a volume of 1 L. Subsequently, a certain quantity of VOCs (chloroform and toluene) was deposited in the gas chamber to form the concentrations range from 2000 to 30 ppm, kept at 40 ℃ for 20 min to allow for complete vaporization and form gas environment for sufficient adsorption before the Raman test. After adsorption, the MOF substrates with adsorbed gas molecules were

removed from the chamber and placed on the microscope stage for SERS measurement under ambient air. Raman spectroscopy signals were obtained using a Raman spectrometer (HORIBA, Japan) with a 532 nm air-cooled $Ar^+$ laser line and the laser power was controlled at ~5 mW. The typical spectral collection condition was set to be 5 s' acquisition time, 20 s' exposure time, and two accumulations.

The reproducibility of the Ti-MOF material on gas sensing was evaluated through adsorption–desorption cycles as follows: first, the MOF material was exposed to toluene vapor at 40 °C for 20 min for adsorption, after which its SERS performance was tested. Subsequently, the toluene-adsorbed sample was placed in a vacuum oven at 70 °C for 2 h to desorb toluene. SERS measurement was then repeated to confirm complete desorption. The sample was again subjected to toluene adsorption under the same conditions, followed by another SERS test. This adsorption-desorption-SERS detection procedure was repeated for 5 cycles to assess the stability and reproducibility of the material.

**1.5 Method of DFT calculations**

DFT calculations were performed using the Vienna Ab initio Simulation Package (VASP)[39] with the Perdew–Burke–Ernzerhof (PBE) exchange–correlation functional[40] within the generalized gradient approximation (GGA). The interactions between core and valence electrons were described using the projector augmented wave (PAW) method and corresponding pseudopotentials.[41] Van der Waals interlayer interactions were evaluated using the Grimme-D3 dispersion correction with Becke−Johnson damping.[42,43] Geometry optimizations were carried out using the conjugate-gradient algorithm with an energy cutoff of 500 eV. The convergence criteria for electronic self-consistency and ionic relaxation were set to $10^{-6}$ eV and 0.02 eV/Å, respectively. The adsorption molecule in MOF crystal was computed using a Γ-centered $3 \times 3 \times 3$ k-point mesh for Brillouin zone sampling. The initial structure of MOF, chloroform and toluene are illustrated in Figure S15.

**1.6 Determination of the enhancement factor (EF).**

According to the methods proposed in the literature,[25] the value of EF (Table S1) can be determined according to equations below:

$$EF = \left(\frac{I_{SERS}}{N_{SERS}}\right)\left(\frac{N_{bulk}}{I_{bulk}}\right) \#(1)$$

$$N_{SERS} = \left(\frac{\rho V_{detect}}{M}\right)\left(\frac{N_A h A_{Raman\ spot}}{V_{container}}\right) \#(2)$$

$$N_{bulk} = \left(\frac{\rho V_{detect}}{M}\right)\left(\frac{N_A h A_{Raman\ spot}}{V_{detect}}\right) \#(3)$$

$$EF = \left(\frac{I_{SERS}}{\left(\frac{\rho V_{detect}}{M}\right)\left(\frac{N_A h A_{Raman\ spot}}{V_{container}}\right)}\right)\left(\frac{\left(\frac{\rho V_{detect}}{M}\right)\left(\frac{N_A h A_{Raman\ spot}}{V_{detect}}\right)}{I_{bulk}}\right)$$

$$= \left(\frac{I_{SERS}}{V_{detect}}\right)\left(\frac{V_{container}}{I_{bulk}}\right)$$

Where the $I_{SERS}$ and $I_{bulk}$ are the intensities of the typical Raman peak (666 $cm^{-1}$ for chloroform ($^{\nu}C-Cl$) and 785 $cm^{-1}$ for toluene ($^{\delta}C=C$)) for the VOCs in the SERS and normal Raman spectra, and $N_{SERS}$ and $N_{bulk}$ are the average number of molecules in the focal spot area for the evaporated and liquid chloroform or toluene. $V_{container}$ is the volume of the quartz container (1 L) used in this experiment, $V_{detect}$ is the volume of the liquid chloroform or toluene (L); $A_{Raman}$ is the laser spot area (10 μm in diameter), $N_A$ is the Avogadro constant, $M$ is the molecular weight and ρ is the density of chloroform or toluene ($g/cm^3$), $h$ is the confocal depth of the laser beam (μm). The values of the parameters are shown in Table S1. Following this validated approach, we calculated the EF using MIL-125-Zn-Toluene as a representative example, as outlined below:

$$EF = \left(\frac{103.34}{8.64 * 10^{-6}}\right)\left(\frac{1}{26.14}\right) = 4.58 * 10^5$$

**Table S1.** The calculation of EF for the samples.

| Substrate | $I_{SERS}$ | $I_{bulk}$ | $V_{detect}$, $\times 10^{-6}$, L | $V_{container}$, L | $EF$($\times 10^5$) |
|---|---|---|---|---|---|
| MIL-125-Chloroform | 139.49 | 27.30 | 6.67 | 1 | 7.66 |

| | | | | | |
|---|---|---|---|---|---|
| MIL-125-defect-Chloroform | 114.33 | 27.30 | 6.67 | 1 | 6.28 |
| MIL-125-Zn-Chloroform | 61.38 | 27.30 | 6.67 | 1 | 3.37 |
| MIL-125-Mn-Chloroform | 41.99 | 27.30 | 6.67 | 1 | 2.31 |
| MIL-125-Cu-Chloroform | 37.22 | 27.30 | 6.67 | 1 | 2.04 |
| MIL-125-Toluene | 65.22 | 26.14 | 8.64 | 1 | 2.89 |
| MIL-125-defect-Toluene | 48.85 | 26.14 | 8.64 | 1 | 2.16 |
| MIL-125-Zn-Toluene | 103.34 | 26.14 | 8.64 | 1 | 4.58 |
| MIL-125-Mn-Toluene | 80.00 | 26.14 | 8.64 | 1 | 3.54 |
| MIL-125-Cu-Toluene | 71.63 | 26.14 | 8.64 | 1 | 3.17 |

## 2. SEM measurements

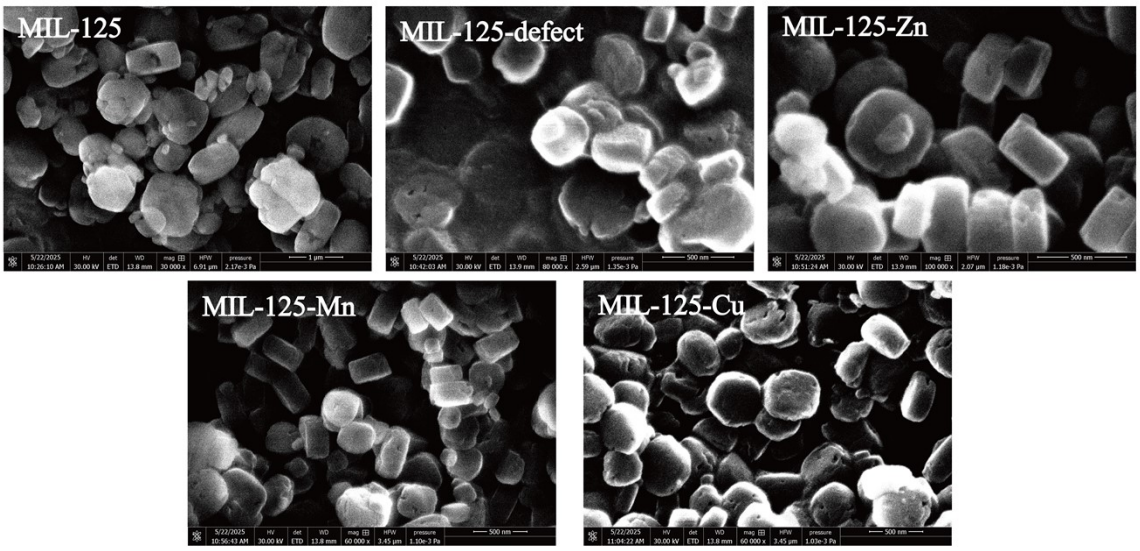


**Figure S1.** SEM images of MIL-125, MIL-125-defect, and MIL-125-X (X=Zn, Mn, Cu).

## 3. EDS measurements

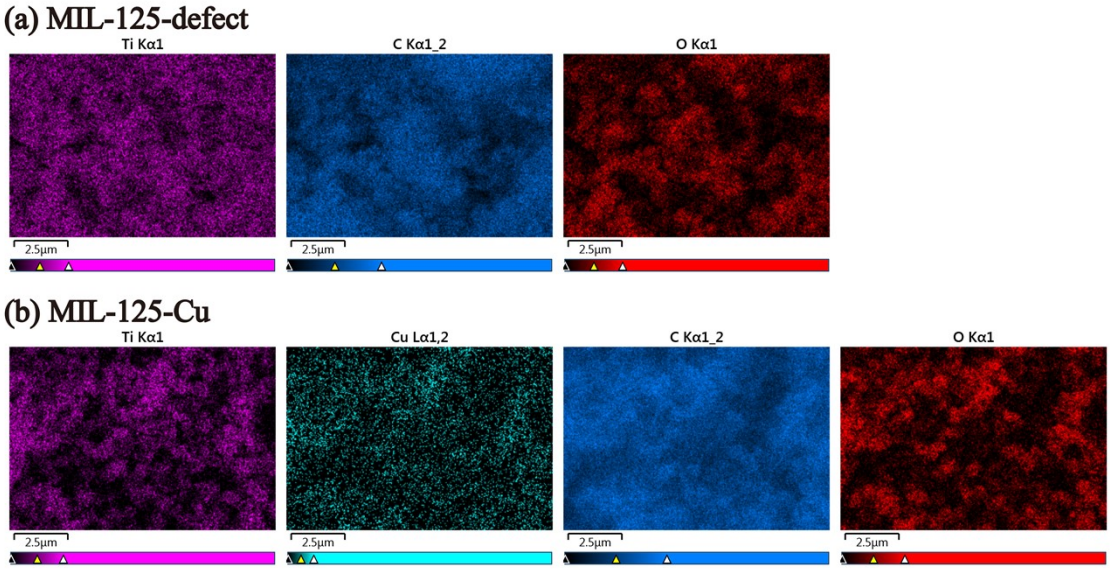


**Figure S2.** Energy Dispersive X-ray spectroscopic (EDS) elemental mapping of (a) MIL-125-defect and (b) MIL-125-Cu.

## 4. XRD and Raman measurements

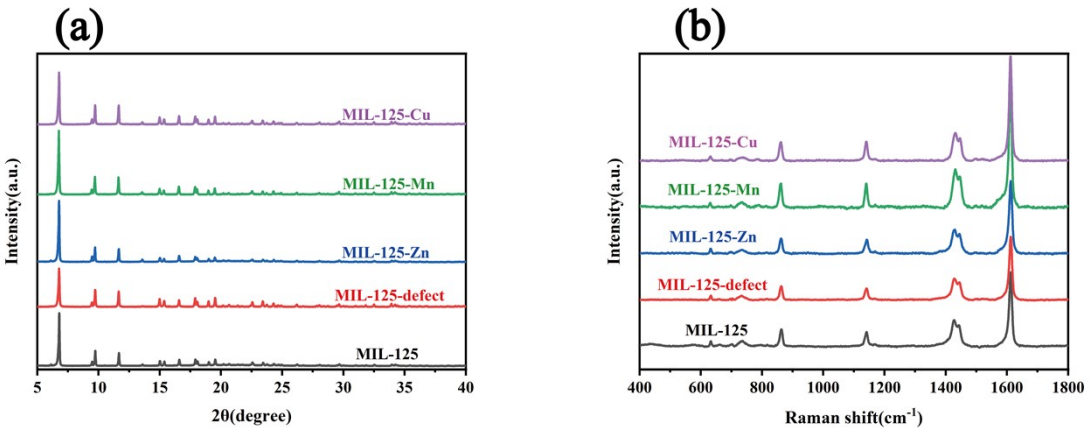


**Figure S3.** (a) XRD and (b) Raman spectra of MIL-125, MIL-125-defect, and MIL-125-X (X=Cu, Zn, Mn).

## 5. FT-IR measurements

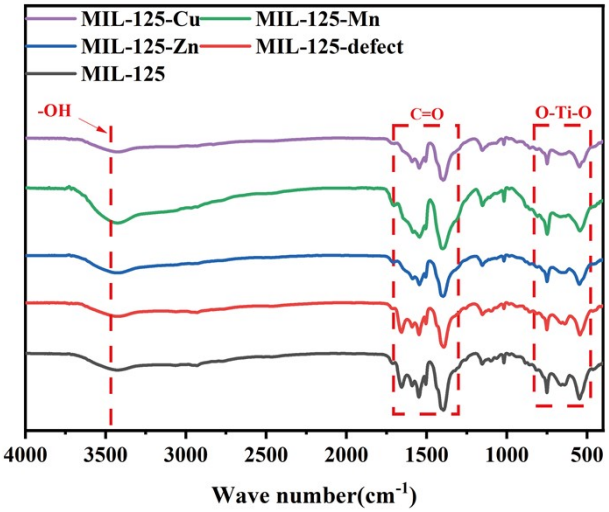


**Figure S4.** FT-IR measurements of MIL-125, MIL-125-defect, and MIL-125-X (X=Cu, Zn, Mn).

## 6. XPS measurements

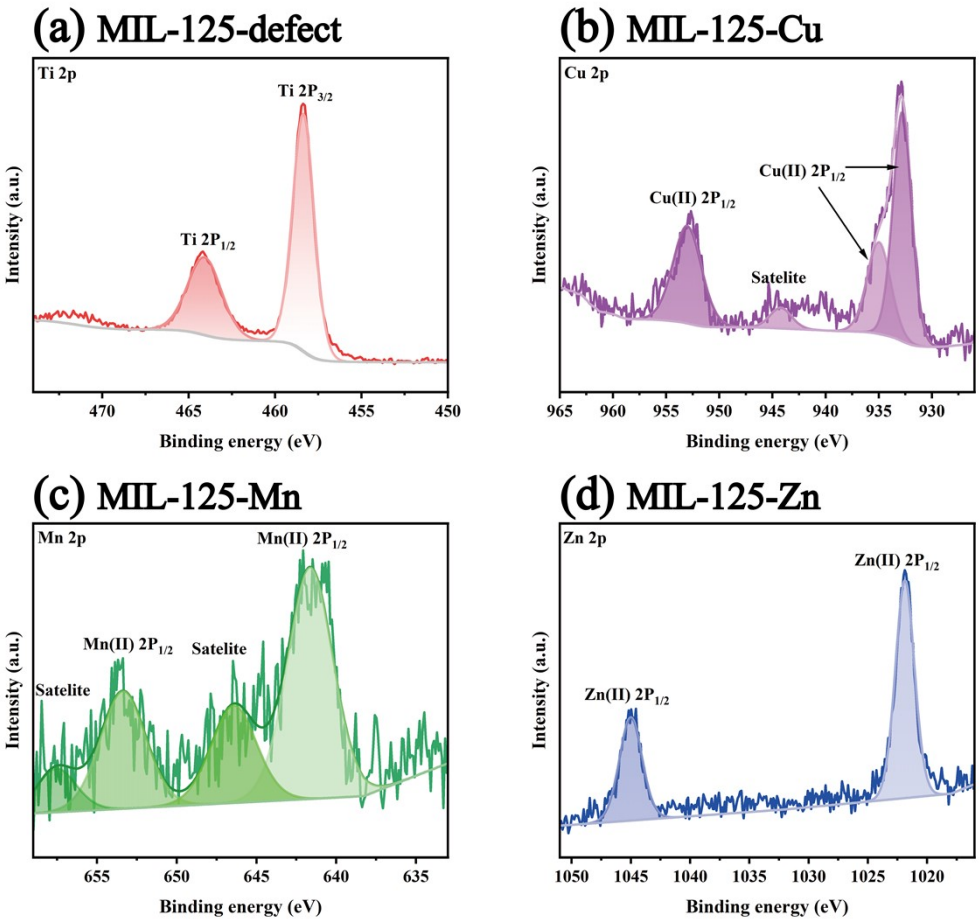


**Figure S5.** X-ray photoelectron spectra (XPS) of (a) MIL-125-defect, (b) MIL-125-Cu, (c) MIL-125-Mn, and (d) MIL-125-Zn. XPS analysis is consistent with the divalent secondary metal sites.

All element spectra adopted the Shirley or linear type background depending on the background slope, and fittings of the peaks were done with CasaXPS software.

## 7. SERS spectra of different ratios of toluene and chloroform mixtures.

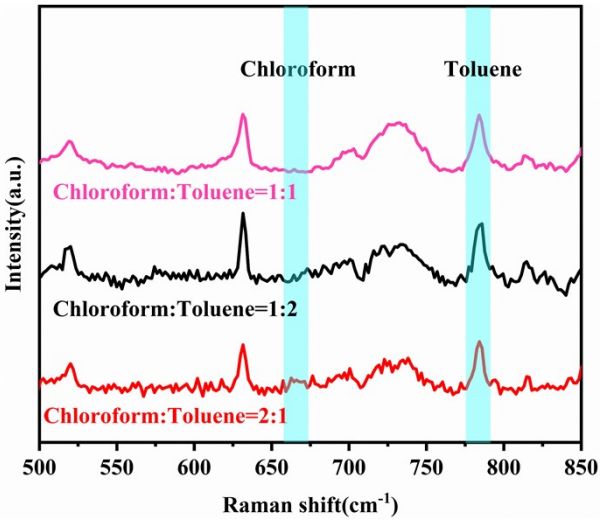


**Figure S6.** SERS spectra of chloroform and toluene mixtures with different ratio of volumes (toluene: chloroform=1:1, 1:2, and 2:1, respectively) adsorbed on Ti-MOF (MIL-125-Zn as an example).

## 8. UV-vis adsorption measurements

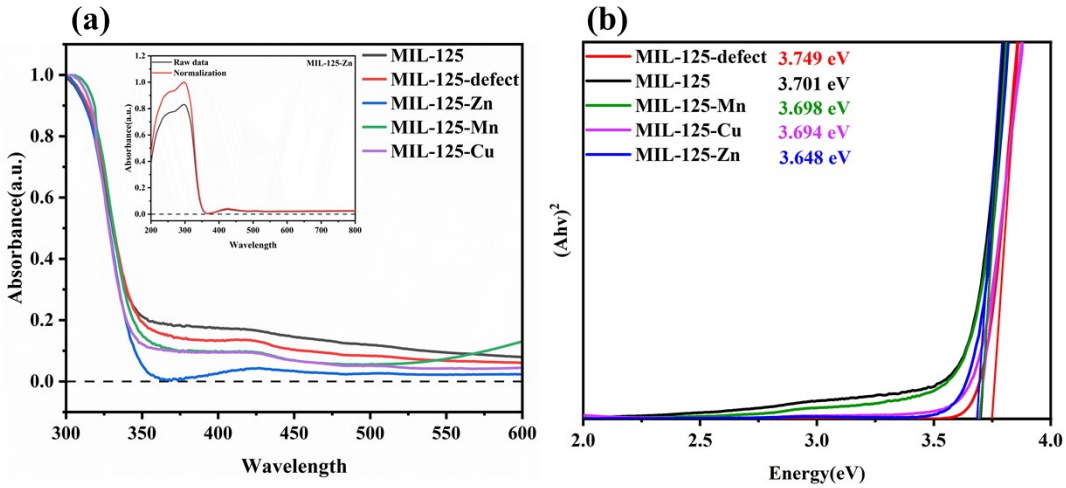


**Figure S7.** (a) UV-vis measurements and the (b) calculated band gaps of MIL-125, MIL-125-defect, and MIL-125-X (X=Cu, Mn, Zn). The data inset (a) represents the original data for MIL-125-Zn (raw data and normalization data).

## 9. Adsorption stability and SERS spectra of gas adsorbed on MIL-125-Cu+Ag

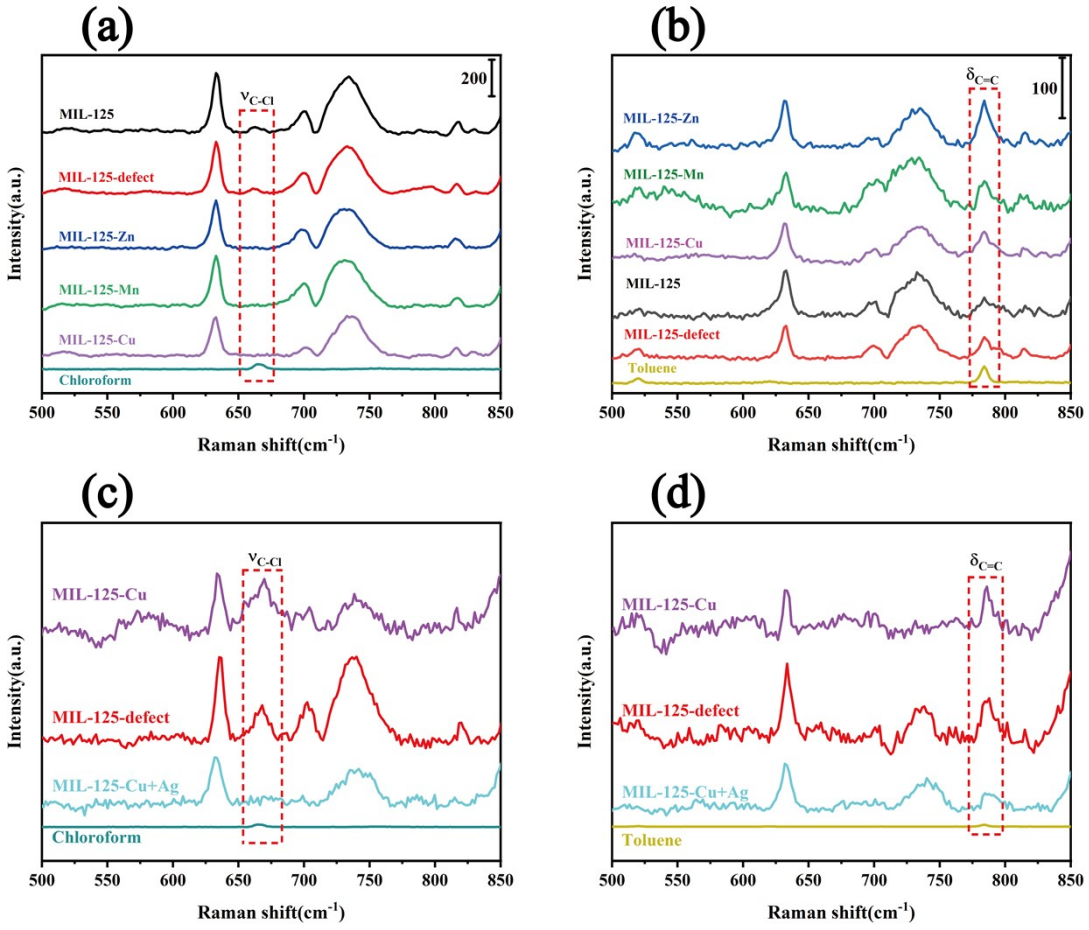


**Figure S8.** SERS spectra of (a) chloroform and (b) toluene adsorbed on MIL-125, MIL-125-defect, and MIL-125-X (X=Cu, Zn, Mn) after 24 h; SERS spectra of (c) chloroform and (d) toluene adsorbed on MIL-125-Cu+Ag with comparison with MIL-125-Cu and MIL-125-defect.

## 10. Stability and reproducibility of Ti-MOF for long-term sensing performances

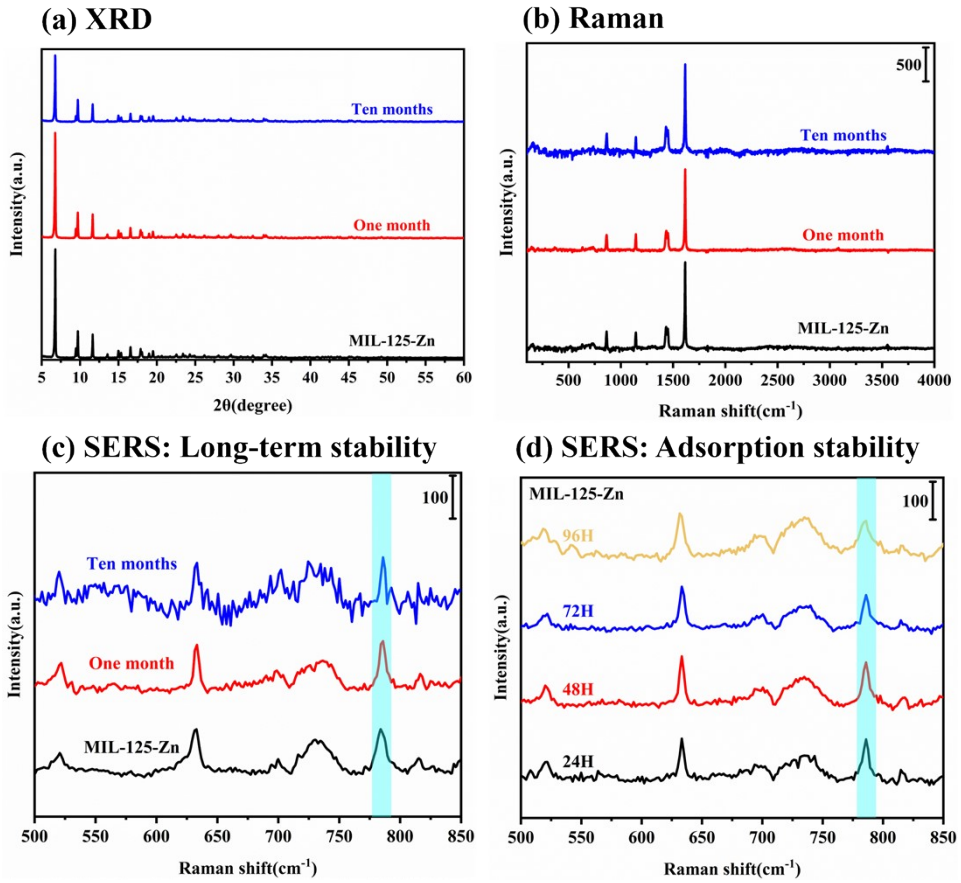


**Figure S9.** (a) XRD and (b) Raman measurements of MIL-125-Zn fresh prepared, prepared one month and ten months ago; (c) SERS measurements of toluene adsorbed on MIL-125-Zn fresh prepared, prepared one month and ten months ago; (d) SERS measurements of toluene adsorbed on MIL-125-Zn after 24, 48, 72, and 96 h.

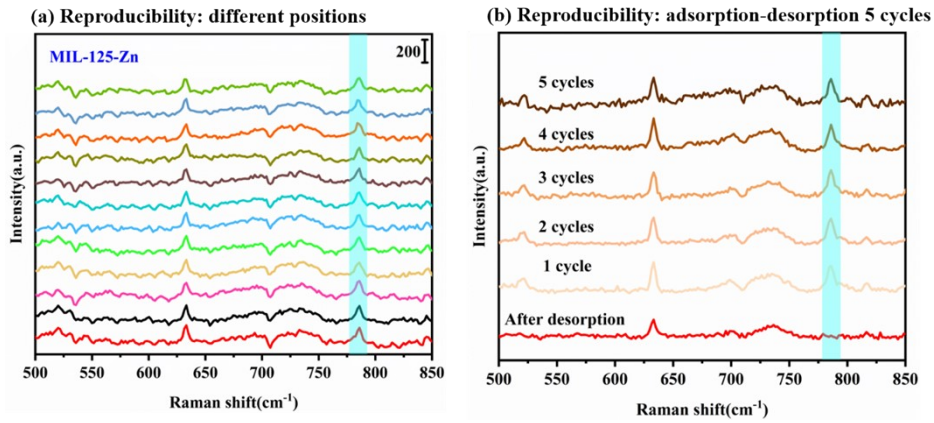


**Figure S10.** SERS measurements for the reproducibility of the Ti-MOF on detecting toluene: (a) measured at 12 different positions; (b) adsorption-desorption of toluene with 5 cycles.

## 11. PL measurements

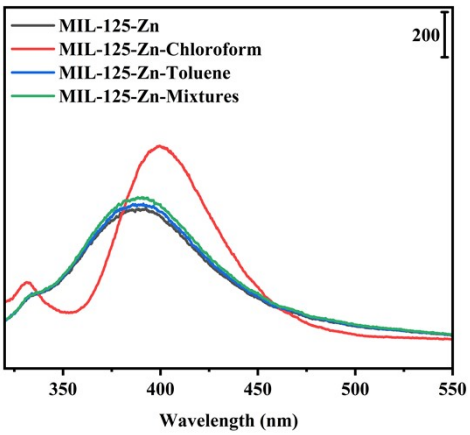


**Figure S11.** PL measurements of MIL-125-Zn and the adsorption of chloroform, toluene, and the mixtures of chloroform and toluene on MIL-125-Zn.

## 12. Limit of detection measurements of chloroform

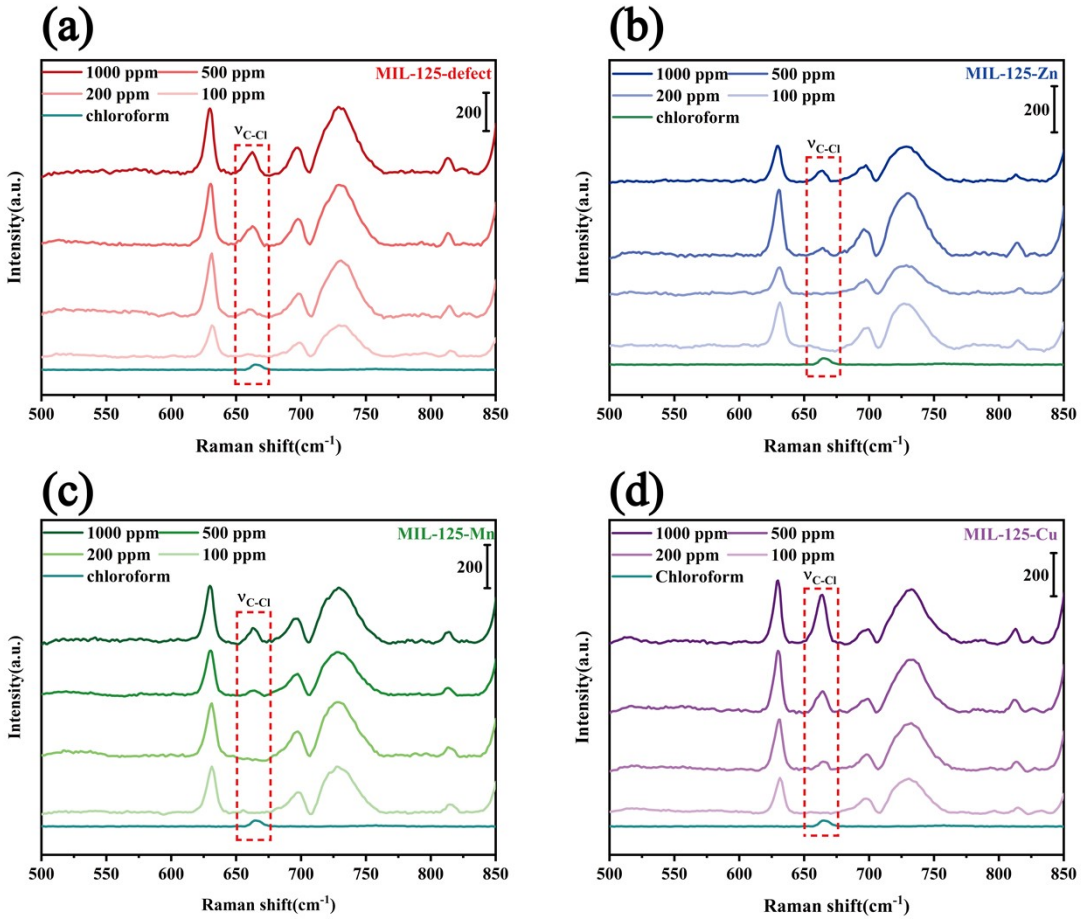


**Figure S12.** SERS spectra of chloroform with different concentrations adsorbed on (a) MIL-125-

defect, (b) MIL-125-Zn, (c) MIL- 125-Mn, and (d) MIL- 125-Cu.

## 13. Limit of detection measurements of toluene

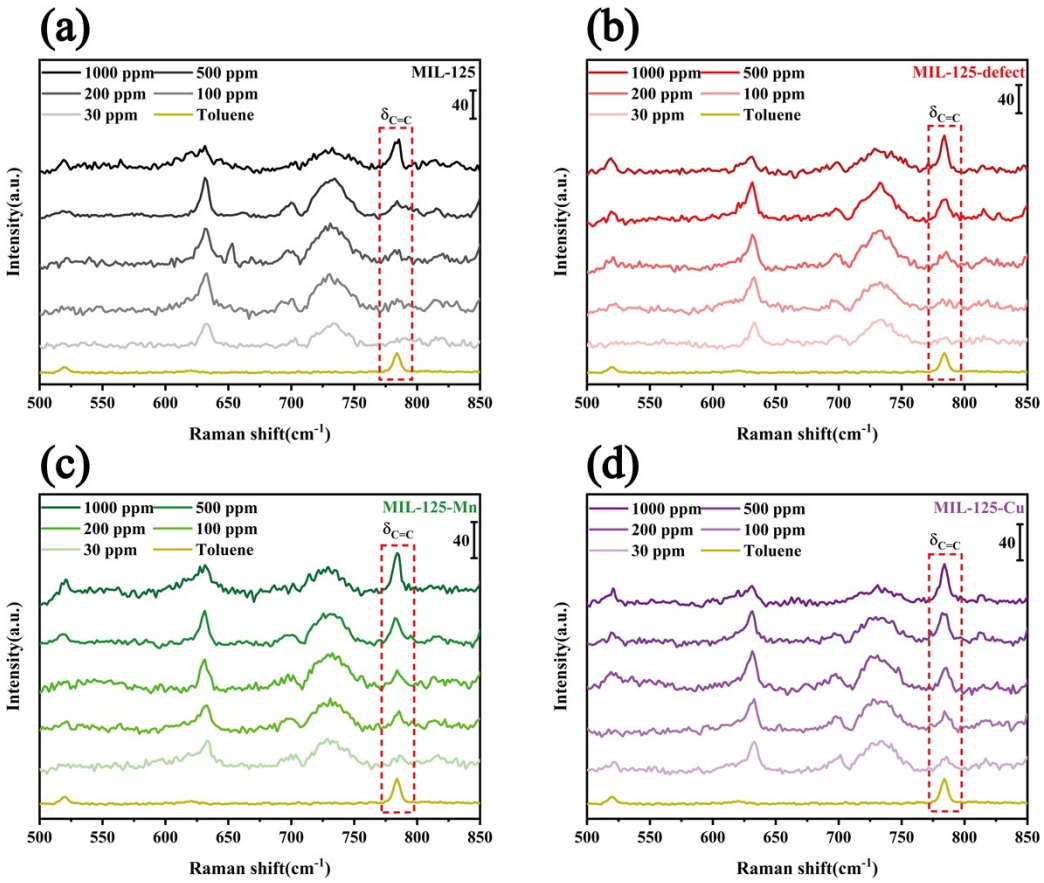


**Figure S13.** SERS spectra of toluene with different concentrations adsorbed on (a) MIL-125, (b) MIL-125-defect, (c) MIL- 125-Mn, and (d) MIL- 125-Cu.

## 14. Raman spectra of dichloromethane and benzene

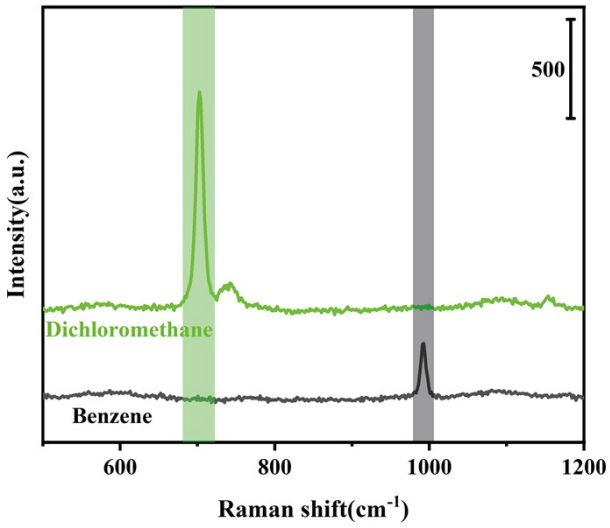


**Figure S14.** Raman spectra of dichloromethane and benzene. Green marked area and dark grey marked area represent the characteristic peak of dichloromethane (C-Cl) and benzene (C=C), respectively.

## 15. Atomic structure of MIL-125, chloroform and toluene

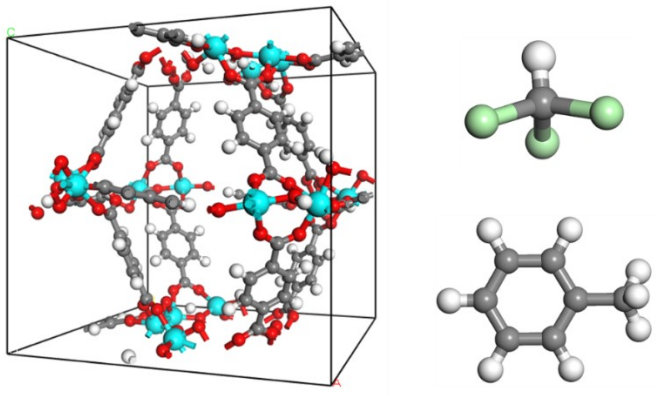

**Figure S15.** The atomic structure of MIL-125, chloroform, and toluene.